The Iraqi Journal For Mechanical And Material Engineering, Vol.20, No4,Dec. 2020

THE EFFECT OF VIBRATION ON NATURAL CONVECTION HEAT TRANSFER IN AN ENCLOSED SQUARE CAVITY

Baydaa Khalil Khudhair [1]
21979@studentuotechnology.edu.iq

Adel Mahmood Salh[2]
adel196150@yahoo.com

[1,2] **University of Technology, Department of Mechanical engineering**

ABSTRACT

A numerical investigation has been implemented to elucidate the effect of vertical and horizontal vibration at normal gravity on natural convection in a square enclosure filled with air at Rayleigh number 7×10^7 and 4×10^8. The enclosure was comprised of two vertical and opposed surfaces (the right hot and the left cold) while the two other surfaces are adiabatic. The two-dimensional, low-Reynolds number $k-\varepsilon$ turbulence model is applied to enable it to cope with low Reynolds number flows. By transforming the equation of (continuity, Navier-Stokes and energy) using finite volume method from differential forms to algebraic forms using SIMPLE algorithm with hybrid scheme dealing with the time term are adopted to solve the governing equations. A computer program in Fortran 90 was built to carry on the numerical solution. Three cases were studied in this work, case I(reaches to steady state and then begins the effect of vibration at each frequency), caseII and caseIII(begin the effect of vibration from the transient at ascending and descending frequencies respectively).After the validity of the present code by comparing results with these of previous study for similar conditions, solutions have been obtained for Prandtle number of 0.7, aspect ratio (A=1). In the high Rayleih number case (Ra=4×10^8), the gravitional thermal convection dominates, and the vibration motion does not enhances the heat transfer remarkably. In contrast, in low Rayleigh (Ra=7×10^7), the vibration thermal convection is dominant, and the vibration enhaces the heat transfer rate significantly. The effect of vertical directional vibration is more powerful in caseII(ascending frequency), when the horizontal directional vibration more effective in case III(descending frequency).

Keywords: Square Enclosure, Mechanical Vibration ,Vertical and Horizontal Directional Vibration, Ascending and Descending Frequency, Interrupted and Continuous Vibrations

تأثير الاهتزاز المسلط على انتقال الحرارة بالحمل الحراري الحر داخل حيز مربع

عادل محمود صالح **بيداء خليل خضير**

الخلاصة

تم تقديم دراسة عددية لتوضيح تأثير الاهتزاز العمودي والافقي عند ظروف الجاذبية الارضية على انتقال الحرارة بالحمل الحراري الحر في غرفة مربعة الشكل, لرقم رايلي 7×10^7 و 4×10^8 . يسخن الجدار العمودي على يمين الغرفة بثبوت كمية الحرارة أما الجدار المقابل له يكون بارد و اما الاسطح الاخرى فتكون معزولة حراريا .

Received : 23-3-2017
Accepted : 21-6-2017

تضمنت الدراسة تأثير الاهتزاز الميكانيكي في ظروف الجاذبية الارضية المسلط عموديا على غرفة مربعة الشكل وذلك من خلال اعداد نموذج رياضي لاجراء الحل العددي لمعادلة الاستمرارية ومعادلتي نافير-ستوكس للزخم باتجاهين ومعادلة الطاقة و معادلتي نموذج ($k-\varepsilon$ Turbulence Model Low Re) للاضطراب, عن طريق تحويل هذه المعادلات باستخدام طريقة الحجوم المحددة (Finite Volumes Mothod) من معادلات تفاضلية الى معادلات جبرية منفصلة يتم حلها اعتمادا على اسلوب الاجراء البسيط (SIMPLE Algorithm) لجريان مضطرب لمائع لاانضغاطي في اتجاهين لحالة عدم الاستقرار لدراسة تأثير الاهتزاز على معدل انتقال الحرارة داخل الغرفة من خلال دراسة خطوط الانسياب و خطوط ثبوت درجة الحرارة,تم بناء برنامج باستخدام لغة فورتران (Fortran 90) لانجاز الحل العددي, ان الحسابات العددية تم تنفيذها باستخدام الهواء كمائع عمل يملأ الغرفة. تردد الاهتزاز المسلط على الغرفة يكون (8-4-2) هرتز عند عدد رايلي 7×10^{7} و (9-6-3) هرتز عند عدد رايلي 4×10^{8}. ان الدراسة انقسمت الى ثلاث مجاميع, المجموعة الاولى تضمنت الوصول الى حالة الاستقرار وبعد ذلك تم تسليط الاهتزاز لكل تردد على حدة (Interrupted Vibrations), المجموعة الثانية (Continuous Vibrations) تضمنت تسليط الاهتزاز منذ بداية التشغيل للمنظومة ولكن الترددات المسلطة تصاعديا لكل اهتزاز فترة زمنية مساوية للاهتزاز الذي قبله, المجموعة الاخيرة تكون مشابه للثانية ولكن الترددات تبدأ تنازليا, بعد التحقق من وثوقية البرنامج الحالي مع دراسات اخرى عند نفس الظروف, عدد برانتل (Pr= 0.7)والنسبة الباعية A=1 , اظهرت النتائج ان تأثير الاهتزاز يقل عند ارتفاع عدد رايلي , وكذلك تاثير الاهتزاز العمودي اكثر فعالية عند حالة التردد التصاعدي والعكس يكون في الحالة الثالثة حيث تردد الاهتزاز الافقي اعلى منه في العمودي عند نفس الترددات.

NOMENCLTURE

Symbol	Description
α	Thermal diffusivity (m^2/s)
A_c	Cross sectional area (m^2)
A	Aspect ratio
β	Thermal expansion coefficient (1/K)
f_r	Frequency(Hz)
T_a	Ambient (atmospheric) temperature(K)
T_h	Temperature of hot surface(K)
T_c	Temperature of cold surface(K)
ΔT	Temperature difference(K)
F	shape factor = $(\frac{2}{\varepsilon}-1)$
$Q_{convection}$	Convection heat transfer rate calculated from energy balance method= $h.A_h(T_h-T_c)$(W)
$h_{L_o i}$	$=\frac{q}{(T_{hi}-T_c)}$ $(W/m^2.K)$
$\bar{h}$	Average heat transfer coefficient(*W/m2.K*)
$Pr=\frac{\vartheta}{\alpha}$	Prandtl Number
$Gr=\frac{g\,\beta_r\,q''_c\,L_x^{\,4}}{k_r\,\vartheta_r^{\,2}}$	Grashof number
$Ra=\frac{g\,\beta_r\,q''_c\,L_x^{\,4}}{k_r\,\vartheta_r^{\,2}}Pr$	Rayleigh Number
$Ra_{vib}=\frac{1}{2}(\frac{b\omega\,\beta_f\,q''_c\,L_x^{\,2}}{K\upsilon})^2\,Pr$	vibrational Rayleigh number
B	Maximum amplitude of vibration (m)
$\omega=2\pi f_r$	Angular frequency of vibration (rad/sec)
g_o	Gravitational acceleration,9.8 (m/s^2)
ν	Kinematics viscosity **(**m^2/s**)**
ρ	Density(kg/m^3)

$Nu = L_o \frac{h_{L_o}}{K_f}$	Local Nusselt number
$\overline{Nu} = \frac{L\bar{h}}{K_f}$	Average Nusselt number
δ	Dimensionless Distance between nodes
ΔV	Dimensionless Volume of control volume
ε	Rate of dissipation of kinetic energy (m^2 / s^3)
Γ	Diffusion coefficient
ϕ	General dependent variable
$\phi_P^{\ n}$	New under-relaxed value
$\phi_P^{\ \circ}$	Previous under-relaxed value
ϕ_P	Obtained under-relaxed value
S_u	Constant part of linearized source term
S_p	Coefficient of ϕ_P in linearized source term
θ	Dimensionless temperature
ϑ	Kinematic viscosity(m^2/s)
Σ	Stephan-Boltzman constant = $5.669*10^{-8}$ (W/k^4m^2)
μ	Dynamic viscosity ($kg/m.s$)
θ	Dimensionless temperature
ω	Dimensionless frequency of vibration
Ω	Angular frequency of vibration (rad/sec)
Π	Constant ratio
T	Time (s)
τ	Dimensionless time

INTRODUCTION

Natural convection in an enclosure has received a great deal of attention in the past, but studies on thermal convection in an enclosure induced simultaneously by gravity and vibration, which is important in material processing (Y. Kamotani *et.al.*, 1981; M. Wadih and B. Roux 1988) or in heat transfer under a vibrational environment(P. D. Richardson,1967) are very rare. A problem of natural convection in an enclosure cavity is important and widely considered in the design of device such as dissipated fins in a heat exchanger and arrays of electric components in a computer. However, in practical situation the devices in the system are always under dynamic situation due to the operation of the system, which results in the device being unavoidably subjected to vibration motion. To validate the mechanism of natural convection on the vibrating enclosure induced by the operation of the system becomes an urgent need for the design of precise and effective device (Fu and Chien 2006) .Vibrations are known to be among the most effective ways of affecting the behavior of fluid system, in the sense of increasing or reducing the convective heat transfer. In the past, numerous relating studies investigated the effect of vibration on the natural convection. The effect of mechanical vibrations, as well as sound waves, on heat transfer from bodies in an infinite atmosphere has been studied by many investigators[5]. The idea of using mechanical vibration as a mean for enhancing the heat transfer has received attention from the early beginning; Lord Rayleigh (1877) first analyzed the streaming flow phenomena, in connection with sound waves. In 1960's, Russian scientists including Gershuni et al., (1963) Zen'kovskaya (1966), and

Simonenko (1972) et al., pioneered the study of vibrational convection,(Yuan,2003). (Forbes et al1970) studied experimentally the thermal convection in a vertical rectangular enclosure filled with water. They varied the vibration frequency and acceleration to find on the heat transfer rate. It was shown that the heat transfer rate was increased by the vibration, especially near the resonant natural frequency of the liquid column contained within the enclosure. The maximum enhancement of heat transfer about 50% was obtained during the experiment. (Ivanova, 1988) studied experimentally the vibration effect on the cooling process of the fluid layer between the concentric cylinders. The results showed that increasing the vibration frequency decreased the cooling time of the fluid. (Fu and Shieh,1992; Fu and Shieh,1993) investigated the natural convection in an enclosure affected by variable acceleration and vibration, respectively. The Nusselt numbers varied with the relating parameters were obtained and concise correlation equations to predict the resonant frequency were derived. (Frank T. Ferguson and Lembit U. Lilleleht,1996) completed the study of thermovibrational convection done (W. S. Fu ,1992and W. J. Shieh,1993) through presenting a model of thermovibrational in a vertical, cylindrical cavity and studied the frequency dependence of the heat transfer rate through the system at Rayleigh numbers, Ra, of 0, $10^4, and\, 10^5$,and vibrational Grashof numbers , Gr_v of $10^5 and\, 10^6$. Results indicated that vibrational convection greatly increased heat transfer rates over the unmodulated case by (7-15%) at $Gr_v = 10^5$ and by (50-65%) at $Gr_v = 10^6$. The observed resonant frequencies seemed to agree reasonably well with the predictions given by the resonance frequency equation:

$$\omega_r = \sqrt{2G_{rv}}.Pr$$

where (ω_r the resonant frequency) derived by (Fu and Shieh,1992)was a useful means of estimating the resonance frequency at low Rayleigh numbers. However, this equation had also been extended to include the effect of the static gravitational field on the resonance frequency and it is appeared that equation

$$\omega_r = \frac{\sqrt{2G_{rv}Pr^2} + \sqrt{2G_{rv}Pr^2 + 2\pi^2 RaPr}}{2}$$

may be more suitable for cases where the Rayleigh number and vibrational Grashof number are somewhat comparable in magnitude. (Ki Hyun Kim ***et al***. ,2001) studied numerically the buoyant convection in a side-heated square cavity of a Boussinesq fluid has served as a benchmark configuration (Y. Kamotani *et.al.*, 1981). The two vertical sidewalls were maintained at different constant temperatures Th and Tc, respectively, and the horizontal walls were insulated. The computed results suggested that the resonance takes place when the frequency of oscillations matches the basic mode of internal gravity oscillations. At the resonance frequency, Nusselt was maximized, which suggests intensification of convection activities in the interior. The oscillation in the vertical direction brings forth mostly quantitative changes, but the changes are more pronounced and qualitative when the oscillation is in the horizontal direction. Wu-Shung Fu and Chien-Ping Huang ,(2006) studied numerically the effects of vibrational heat surface on the natural convection in a vertical channel flow. The results showed that for the same Rayleigh number, the natural convection of a vibration heated plate with a certain combination of frequency and amplitude was possibly smaller than that a stationary state. More heat transfer rate of the heated plate obtained when the frequency was larger than the critical frequency and for the same Rayleigh number and amplitude conditions, and the situation of which the frequency is larger than the critical frequency is advantageous to the heat transfer and vice versa. Hideshi Ishida ***et al.*** ,(2012) proposed a method to obtain a forced oscillation induced by an arbitrary small time-

varying force on a stable thermal convection field, and a framework for finding universal and inherent resonance modes on the field , independent of the ways of forced vibration , indicators of resonance and other information. The method also provided indicators to quantify the efficiency in realizing a given resonant mode by a specific forced vibration. Ahadi *et al*. (2014) experimentally studied the effects of different parameters of vibrational forces, such as frequency and amplitude on the influences of a wide range of vibration Rayleigh or on the measurement of thermo-diffusion in a microgravity environment subjected to a constant temperature difference between two walls of cubic cavity. And they investigated the impacts on the separation of the components of the mixture due to the change in the forced vibration from low to high vibration Rayleigh number. The ISS (The International Space Station) experimental data were obtained using an optical digital interferometry in a reduced gravity environment. The experiment was performed in a cubic cell containing an aqueous solution exposed to 10 K temperature gradient. Different runs of a water and isopropanol mixture with a negative Soret coefficient and the same temperature difference were chosen as test cases. The results showed maximum separation and Soret coefficient for the case with minimum Rayleigh number, a linear relation between the vibration Rayleigh number and the maximum separation was not detected. This is unexpected since most often the increase in Rayleigh number corresponds to a decrease in the separation of components. Consequently, the aim of this study is to investigate numerically the detailed heat transfer mechanism of thermal convection which is induced by gravity and vibration simultaneously in a square enclosure at three cases and in vertical and horizontal directional of vibration. CaseI (reaches to steady state and then begins the effect of vibration at each frequency), caseII and caseIII(begin the effect of vibration from the transient at ascending and descending frequencies respectively) caused by abrupt change of the wall temperature and vibration conditions. Based upon the results of Adel M. Salh *et al*. (2014), the phenomena for a Rayleigh number of 7×10^{7} influenced by the vertical vibration are more remarkable than those for a Rayleigh number of 4×10^{8}; the case for Rayleigh numbers of 7×10^{7} and 4×10^{8} are then preliminarily studied and the vibrational Rayleigh number at each frequency and the dimensionless frequency of vibration at the table 1. Since in this case there are many factors that affect the heat transfer mechanism and the vibration perpendicular to the temperature gradient is the most critical. Mainly consider the effects of vertical and horizontal vibration frequency on heat transfer mechanism corresponding to the variations of vibration frequency from low to high frequency at case of interrupted vibration (reach to steady state then begin the effect of vibration), and at the case of continuous vibration (at ascending frequencies and descending frequencies from start of operating the system). The time history of the steam lines, isothermal lines and Nusselt number are also presented.

Rayleigh number	Frequency(fr)Hz	Dimensionless frequency(ω)	Vibrational Rayleigh number
7×10^{7}	2	1.257	2×10^{4}
7×10^{7}	4	2.513	3×10^{5}
7×10^{7}	8	5.02655	2×10^{6}
4×10^{8}	3	0.57	7×10^{6}
4×10^{8}	6	1.13	4×10^{7}
4×10^{8}	9	1.7	1.6×10^{8}

MATHMETICAL AND NUMERICAL MODEL

The physical model sketched in figure (1) is an air-filled (*Pr=0.71*) square enclosure (constant property) with two horizontal adiabatic walls and the right wall is heated at constant heat flux, where the left wall is cooled at constant temperature Tc. Initially (t=0), the fluid in the enclosure is stationary and the temperature of the fluid and vertical walls is kept at Tc. After wards ($t^{>0}$), the vertically downward constant gravity is g_o, and two cases are considered for the fluctuating part of acceleration: (case1),in the horizontal direction $g_x = \rho\beta(T - T_c)\left(b\Omega^2 sin\Omega t\right)$ and the non-dimensional in the x- direction $g_x = \theta\omega\sqrt{2Ra_{vib}\,Pr}\sin\omega t$; (case2), in the vertical direction $g_y = \rho\beta(T - T_c)\left(g_o + b\Omega^2 sin\Omega t\right)$ and the non-dimensional in the y-direction $g_y = \theta(1 + \omega\sqrt{2Ra_{vib}\,Pr}\sin\omega\tau)$. Then a non-inertial frame of reference traveling with the enclosure is used and parameters b, Ω and t are respectively the displacement amplitude, angular frequency and time.

In order to facilitate the analysis, the following assumptions are made:

1. Constant heat flux at the wall.
2. The fluid is Newtonian, unsteady, and the flow is turbulent, $Ra^{>10^6}$. (G. Barakos, E. Mitsoulis and D. Assimacopoulos,1994).
3. The vibration velocity amplitude (b Ω) is not large, and the flow is assumed to be incompressible.
4. fluid properties are constants and fluid density variations are neglected except in the buoyancy term (Boussinesq approximation).
5. Two dimensional distribution of fluid flow and temperature and the gravity acts in the vertical direction.
6. Viscous dissipation and radiation effect is neglected, and no heat generation inside enclosure.

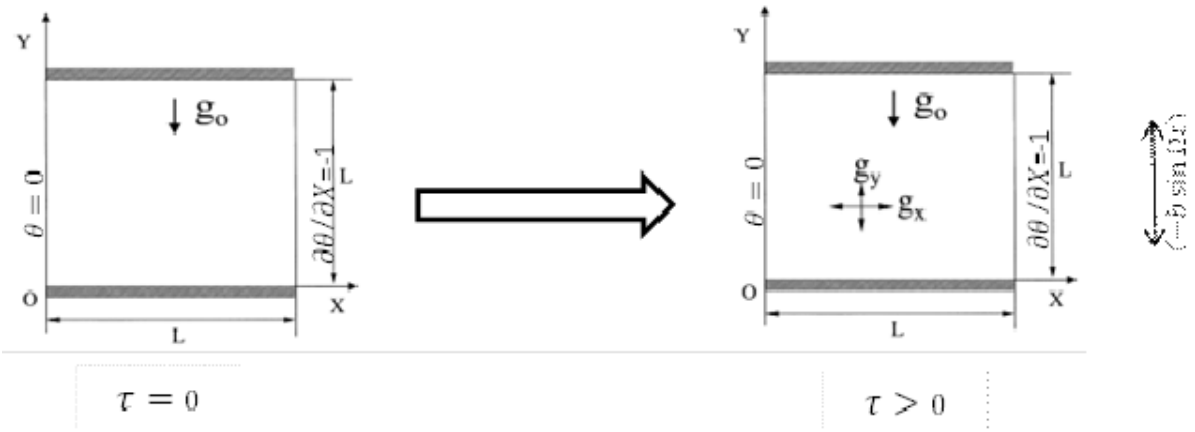

Fig.(1) Physical Model

With these assumptions, the Reynolds equations for a Boussinesq incompressible fluid under unsteady state conditions. The basic conservation and governing time-dependent equations can be written in nondimensional form as follows:

1. The continuity equation for the unsteady state and incompressible flow is given by:

$$\frac{\partial U}{\partial X} + \frac{\partial V}{\partial Y} = 0 \qquad (1)$$

2. The governing time-depended Navier-Stokes equations two-dimensional,

$$\frac{\partial U}{\partial \tau}+U\frac{\partial U}{\partial X}+V\frac{\partial U}{\partial Y}=-\frac{\partial P}{\partial X}+\sqrt{\frac{Pr}{Ra}}\frac{\partial}{\partial X}\left[(\mu^*+\mu_t^*)\left(2\frac{\partial U}{\partial X}\right)\right]+\sqrt{\frac{Pr}{Ra}}\frac{\partial}{\partial Y}\left[(\mu^*+\mu_t^*)\left(\frac{\partial U}{\partial Y}+\frac{\partial V}{\partial X}\right)\right]+\theta \quad (2)$$

$$\frac{\partial V}{\partial \tau}+U\frac{\partial V}{\partial X}+V\frac{\partial V}{\partial Y}=-\frac{\partial P}{\partial Y}+\sqrt{\frac{Pr}{Ra}}\frac{\partial}{\partial Y}\left[(\mu^*+\mu_t^*)\left(2\frac{\partial V}{\partial Y}\right)\right]+\sqrt{\frac{Pr}{Ra}}\frac{\partial}{\partial X}\left[(\mu^*+\mu_t^*)\left(\frac{\partial U}{\partial Y}+\frac{\partial V}{\partial X}\right)\right]$$
$$+\left[1+\omega Pr\sqrt{2Gr_{vib}}\,\sin\omega t\right] \quad (3)$$

4. The energy equation is:

$$\frac{\partial \theta}{\partial \tau}+U\frac{\partial \theta}{\partial X}+V\frac{\partial \theta}{\partial Y}=\frac{1}{\sqrt{\Pr Ra}}\frac{\partial}{\partial X}\left[\left(\mu^*+\frac{\mu_t^* Pr}{\sigma_T}\right)\left(\frac{\partial \theta}{\partial X}\right)\right]+\frac{1}{\sqrt{\Pr Ra}}\frac{\partial}{\partial Y}\left[\left(\mu^*+\frac{\mu_t^* Pr}{\sigma_T}\right)\left(\frac{\partial \theta}{\partial Y}\right)\right] \quad (4)$$

Turbulence modeling (Low Re $k-\varepsilon$ turbulence model)

Different turbulence models are used to predict the natural convection heat transfer inside enclosed cavity. One of the widely used models of turbulence is the $\text{Low Re}\,k-\varepsilon\,\text{Turbulence Model}$ applied to enable it to cope with low Reynolds number flows. The wall damping function is applied to ensure that viscous stresses take over from turbulent Reynolds stresses at low Reynolds numbers and in the viscous sub-layer adjacent to solid walls Launder and Sharma (1974). (Sohail Anwar,2003)

In the above equations all Reynolds stresses are incorporated into the diffusion terms using a turbulent viscosity equation at non-dimensional

$$\mu_t^*=\sqrt{\frac{Ra}{Pr}}\rho^*\,C_\mu\,f_\mu\,\frac{K^2}{\varepsilon} \qquad \text{(Baydaa Khalil Khudhair, 2015)} \quad (5)$$

Where C_μ is a constant and K and ε are calculated from their transport equations

5. The non-dimensional turbulence kinetic energy (*K*- equation)

$$\rho^*\frac{\partial K}{\partial \tau}+\rho^*U\frac{\partial K}{\partial X}+\rho^*V\frac{\partial K}{\partial Y}=\sqrt{\frac{Pr}{Ra}}\frac{\partial}{\partial X}\left[\left(\mu^*+\frac{\mu_t^*}{\sigma_k}\right)\left(\frac{\partial K}{\partial X}\right)\right]+\sqrt{\frac{Pr}{Ra}}\frac{\partial}{\partial X}\left[\left(\mu^*+\frac{\mu_t^*}{\sigma_k}\right)\left(\frac{\partial K}{\partial X}\right)\right]$$
$$+P_K+G_K-\rho^*\varepsilon^* \quad (6)$$

6. The non-dimensional turbulence dissipation (ε- equation)

$$\rho^*\frac{\partial \varepsilon^*}{\partial \tau}+\rho^*U\frac{\partial \varepsilon^*}{\partial X}+\rho^*V\frac{\partial \varepsilon^*}{\partial Y}=\sqrt{\frac{Pr}{Ra}}\frac{\partial}{\partial X}\left[\left(\mu^*+\frac{\mu_t^*}{\sigma_\varepsilon}\right)\left(\frac{\partial \varepsilon^*}{\partial X}\right)\right]+\sqrt{\frac{Pr}{Ra}}\frac{\partial}{\partial X}\left[\left(\mu^*+\frac{\mu_t^*}{\sigma_\varepsilon}\right)\left(\frac{\partial \varepsilon^*}{\partial X}\right)\right]+(C_{\varepsilon 1}\,f_1(P_K+C_{\varepsilon 3}\,G_K)-$$
$$\rho^*C_{\varepsilon 2}\,f_2\,\varepsilon^*)\frac{\varepsilon^*}{K} \quad (7)$$

The non-dimensional equation represents the rate of generation of turbulent kinetic energy due to mean velocity gradients P_K and G_K generation of turbulent kinetic due to buoyancy is:

$$P_K=\mu_t^*\sqrt{\frac{Pr}{Ra}}\left(2\left(\frac{\partial U}{\partial X}\right)^2+2\left(\frac{\partial V}{\partial Y}\right)^2+\left(\frac{\partial U}{\partial Y}+\frac{\partial V}{\partial X}\right)^2\right) \quad (8)$$

$$G_K=\frac{1}{\sqrt{\Pr Ra}}\frac{\mu_t^*}{\sigma_T}\frac{\partial \theta}{\partial y} \quad (9)$$

In addition, there are some extra terms, denoted by $k-\varepsilon$ equation to account for near wall behavior. f_μ and f_2 are wall damping functions which occurs when low Reynolds number turbulence models are used. σ_k is the turbulent Prandtl number ($\sigma_k=Pr_t$) for ε Launder and Spalding(1972) .(E. Papanicolaou and V. Belessiotis, 2005). The values are empirical constants used in $\text{Low Re}\,k-\varepsilon\,\text{Turbulence Model}$ as detailed in table (2).

$$f_\mu = exp\left[\frac{-3.4}{(1+Re_t/50)^2}\right] \quad (10)$$

C_μ	$C_{\varepsilon 1}$	$C_{\varepsilon 2}$	$C_{\varepsilon 3}$	σ_k	σ_ε	σ_T	f_1
0.09	1.44	1.92	tanh |V/U|	1.0	1.3	0.9	1.0

$$f_2 = 1 - 0.3\exp\left(-Re_t^{\,2}\right) \quad (11)$$

Table (2) constants used in low Re $k-\varepsilon$ Turbulence Model $(Lander-Sharma)$. (S. V. Patankar, 1980)

The turbulent Reynolds number in terms of dimensionless variables is

$$Re_t = Pr\frac{K^2}{\varepsilon\theta} \quad (12)$$

Boundary and Initial Conditions:

In this work, a uniform heat flux condition is imposed at the heated walls and in accordance with Fig. 1, the boundary conditions of the problem appear as follows :

$\tau = 0 \qquad U = V = 0$

$\tau > 0$

$X = 0 \quad U = V = 0, \theta = 0$

$X = l \quad U = V = 0, \left(\frac{\partial\theta}{\partial x}\right)_{x=l} = -1$

Y=0 and Y=l, U=V=0, $\partial\theta/\partial y=0$ (13)

For the turbulence variables in $(Lander-Sharma)$ model the following values are specified at the wall:

$$k_w = 0 \quad ,\varepsilon_w = 2Pr\left(\frac{\partial\sqrt{K}}{\partial n}\right)^2 = 2Pr\frac{K_{w+1}}{(\Delta n)^2}\,[19] \quad (14)$$

Where Δn is the normal wall distance of the first node.

By using these dimensionless variables below the continuity, momentum, thermal energy turbulent kinetic energy and rate of energy dissipation equations become at the form :

$$X,Y = \frac{x,y}{L} \;;\; U,V = \frac{u,v}{u_{ref}} \;;\; P = \frac{p}{\rho\, u_{ref}^2} \;;\; \theta = \frac{(T-T_c)k_{cond}}{q"L};$$

$$;\; ;\tau = \frac{t\, u_{ref}}{L}; \omega = \frac{\Omega L}{u_{ref}}; \rho^* = \frac{\rho}{\rho_{ref}} \;;$$

$$u_{ref} = \sqrt{\frac{g\beta q"L^2}{k_{cond}}}; \; Ra = \frac{\rho^2 g_o \beta q"L^4}{k_{cond}\,\mu^2}Pr \;;\; Pr = \frac{\nu}{\alpha} = \frac{\mu C_p}{k_{cond}};$$

$$Gr_{vib} = \frac{1}{2}\left[\frac{\rho^2(b\Omega)\beta q"L^2}{k_{cond}\,\mu^2}\right]^2 \quad (15)$$

$$Ra_{vib} = \frac{1}{2}\left[\frac{\rho^2(b\Omega)\beta q"L^2}{k_{cond}\,\mu^2}\right]^2 Pr \quad (16)$$

The local heat transfer from the heated wall to the air stream depends on the temperature gradient at the cold or hot wall. The convective heat flux from the wall to the air stream can be expressed in terms of the local (h) as:

$$h = \frac{q''}{(T_h - T_c)}, at\ y = o\ and y = l \quad (17)$$

For the purpose of generalizing the heat transfer results, the local Nusselt number is calculated by the following equation:

$$Nu_y = \frac{h l_{ref}}{k_{cond}} = \frac{q'' l_{ref}}{\left(T_{h_{(0,y)}} - T_c\right) k_{cond}} = \frac{1}{\theta(0,y)} \quad (18)$$

$at\ y = o\ and\ y = l$ .Here $l_{ref} = L(length\ of\ the\ cavity).$

The average Nusselt number on the heat surface is expressed as follows:

$$\overline{Nu} = \frac{1}{A_c}\int_0^{A_c} Nu_y\, dY \quad (19)$$

Or

$$\overline{Nu} = \frac{1}{A_c}\int_0^{A_c} Nu_x\, dX \quad (20)$$

The time-averaged Nusselt number per cycle is defined by

$$\overline{Nu} = \frac{1}{\tau_p}\int_0^{\tau_p} Nu d\tau \quad (21)$$

In which τ_p is a periodical time

Such a model has also been used for solving two-dimensional problems . For a sampling of the defining equations used finite volume method . System of algebraic equations is solved by the sweep method implicitly by the linear Gaussian elimination scheme . For the approximation of the convective terms in the equations of motion and energy used hybrid scheme. Developed a computer program (FORTRAN 90) to obtain numerical results using the pressure - velocity coupling (algorithm SIMPLE).A non-uniform grid (81$\times$ 81) mesh network was deployed with the implementation of grid stretching. Because of this crude conjugation and nonlinear equations for convergence procedure is required relaxation. Relaxation factors used for the components of velocity, temperature , pressure, turbulence kinetic energy and dissipation rate , which are, respectively , 0.3 , 0.5, 0.5, 0.7 and 0.7.Figure (2)presents a flow chart for the present code.

TESTING OF THE MODEL:

To assess the validity of the numerical computations and the experimental results were obtained from (Adel M. Salh *et al*. ,2014), of the time-averaged Nusselt number $\overline{Nu}$ which studied the effect of vertical vibration in cubic enclosure. Working fluid was air (Pr=0.71) with aspect ratio (A=1). At Rayleigh number Ra=7$\times$ 10^7 and Ra=4$\times$ 10^8. Numerical results were compared with the vertical vibration at the same frequencies at each Rayleigh number. Figure (3A) (a and b) reveal the effect of vertical vibration for case II (ascending frequencies) and case III(descending frequencies) at Ra=7$\times$ 10^7. Figure (3B) (c and d) reveal the effect of vertical vibration for case II (ascending frequencies) and case III(descending frequencies) at Ra=4$\times$ 10^8. The agreement results between the two works were good.

The validation of the present numerical results of the time histories for the streamlines and temperature contours were used to compare with the numerical results of (Ki Hyun Kim ***et al***. ,2001).The computational results of the vertical vibration from starting at $\omega = 0.66$ and Ra=10^7 are exemplified in figure (4) A and B.

RESULTS OF CALCULATIONS AND DISCUSSION

In order to have insight of the cyclic variations in the flow and thermal fields caused by the vibration of the enclosure, a number of snapshots of the velocity and temperature distributions in a cycle for case I are shown in figures(5,6,7and8). The flow field is illustrated by plotting the velocity vectors, and the thermal field by plotting the isotherm. Figures (5and7) A,B,C reveal the time histories of flow and temperature contours .The effect of vibration on natural convection on vertical and horizontal direction respectively for the frequencies (2,4 and 8)Hz for the case I at Ra=7×10^{7}. From figures (5-A) and (8-A), the thermovibrational convection is weak due to the low vibration Rayleigh number; therefore, the effect of vibration fluid flow is remarkable even for the low frequency situation. In figure (5and6) B,C, two consecutive vibration periods are combined as a period of fluid flow. It is clearly seen that the vibrational Rayleigh number increases, the flow tends to break up from the single loop into two loops. The isotherms increasing does not only gather densely near the higher and lower regions of the left and right walls, respectively, but also along the isotherms gather densely near the vertical walls as a result of increasing vibration frequency, and the thermovibrational convection is dominant. The flow intensity is also substantially increased at increased Rayleigh vibration number as a result of increasing vibration frequency at two amounts of Rayleigh number, the fluid flows mainly in the counterclockwise direction like a rotating flow around the core region. When the Rayleigh number increased to Ra=4×10^{8} , the same behavior of flow and thermal characteristics are observed. Figures (7and8) show the variations in velocity and temperature distributions in case I for the two directions vibration in vertical and horizontal at the frequencies (3.6and9)Hz. In the cyclic process, it is found that the temperature distribution in the enclosure space is appreciably altered by the variation of the vibration for all frequencies. The thermal field experiences a remarkable change as the vibration frequency elevated. For a lower-frequency, the flow in the enclosure is driven mainly by the buoyancy. The fluid in the area adjacent to the hotter right wall moves upwards and that adjacent to the colder left wall moves downwards. Therefore, a flow recirculation is formed in the enclosure. The location of the center of the flow recirculation is not steady but varied with time. As the vibration frequency is increased to be 8Hz or 9Hz, the flow in the enclosure is dominated by the inertia effects from the movement of the vibration enclosure.

When the direction of the vibration changed to horizontal direction, different flow and thermal characteristics are observed. Figure (6and8) show the variations in velocity and temperature distributions in the enclosure under horizontal vibration situation at case I. The dependence of the temperature distribution on the vibration frequency can be observed. A large flow recirculation is produced in the enclosure at low vibration frequency of fr=2Hz at Ra= 7×10^{7} and vice versa at Ra=4×10^{8} at high frequency fr=9Hz. The symmetric pattern was significantly shifted to an asymmetric pattern with a flow recirculation due to the enclosure vibration even at fr=2and3Hz. The flow recirculation moves vortices move up-and-down. The local density of the isotherms adjacent to vertical walls is lower at fr=2Hz than at fr=8Hz. this implies that the thermal boundary layers are thicker and hence the heat transfer rate on the vertical walls is lower at fr=2Hz at Ra= 7×10^{7}. Again, as the vibration frequency is increased to be 4Hz, the flow recirculation is not visible. At Ra=4×10^{8} the boundary layer thicker is increased at increased of vibration frequency and the heat transfer rate on the vertical walls is lower at fr=8Hz. As discussed, the (vertical and horizontal) vibration influence on the vertical and horizontal velocity components (VandU) distribution at the horizontal mid-plane for Ra=7×10^{7} and 4×10^{8} respectively. There is a four set of figures illustrate the effect of vibration on the behavior of flow within the cavity in case I and case II. From the figures (9 Aand B),(10 AandB), it will be noted the change in the direction on vibration from vertical to horizontal have a major influence on flow structure as well as the change in Rayleigh number .From these figures there is a deformation occurs when the directional of vibration was

changed from the vertical to horizontal direction, and there is acceleration of the fluid near the heated wall whereas a strong deceleration near the cold wall. The recirculation zone is created by cold fluid which tends to descend with greater density than the hot fluid under the effect of directional vibration. A change in a local Nusselt number along the hot and cold walls within the cavity in case I is shown in figures (11AandB) at the vertical mid-plane for Ra= 7×10^{7} and 4×10^{8} respectively. Clearly Nu_H is generally increased at the vertical vibration more than the Nu_H horizontal at same case I. Heat transfer enhanced to about 30%, and the Nu_C on both vertical and horizontal vibration at Ra= 7×10^{7} is the same. A less distinctive is visible in Nu_H and Nu_C at Ra=4×10^{8} at directional vibration in vertical and horizontal for case I, heat transfer enhanced to about 16% at vertical than the horizontal vibration. To comparisons of the results of time-averaged Nusselt numbers $\overline{Nu}$ at stagnation (without vibration) with the horizontal and vertical vibration for case I at figures(12AandB) and (13AandB), reveal the effect of vibration at natural convection heat transfer in square cavity at Ra=7×10^{7} and 4×10^{8} respectively. In figure (12-A) at Ra= 7×10^{7} and due to vertical vibration (case I) of the square cavity, the average Nusselt numbers vary periodically and are larger than that stationary state (without vibration motion) completely. At the vibrational motion for each frequency (2and4)Hz the time-average Nusselt numbers increased gradually. At frequency increases to8Hz, the time-averaged Nusselt numbers increased and closed to that fr= 4Hz to the through. In figure (12-B) at Ra= 7×10^{7} and due to horizontal vibration (case I) on the square cavity, the time-average Nusselt numbers vary periodically, and more the vibrational frequency is, the larger $\overline{Nu}$ becomes. At fr=2Hz, most of the average Nusselt numbers are smaller than that stationary state completely, and at fr=(4and8)Hz the average Nusselt numbers are close to each other and close to that stationary state to the through.At vibrational frequencies (3,6and9)Hz, as Rayleigh number increases to 4×10^{8} , the effect of vibration motion in vertical direction (case I) shown in figure(13-A), which is much larger than that indicated in the cases mentioned earlier and the time-average Nusselt number $\overline{Nu}$ begins to be larger than that stationary state. Since the higher Rayleigh number situation means the natural convection to be drastically, the vibrational motion then should be larger in order to lead the time-average Nusselt number of vibration to be more than that of stationary state. The time-average Nuselt numbers begin to be more than the stationary state, and the variations are closed to each other to the through at the frequencies (3and6)Hz. accompanying with the increase of Rayleigh number shown in figure(14-A), the values of fr=9Hz which cause the time-average Nusselt numbers to exceed those of the stationary state and become larger the frequencies(3and6)Hz respectively. Due to horizontal vibration motion of the square cavity of frequencies (3,6and9)Hz shown in figure(13-B), (case I) then for Ra=4×10^{8}, the time average Nusselt numbers are further smaller than the stationary state at each frequency and not exceeded to that of stationary state finally.The comparison between the vertical and horizontal vibration for ascending frequencies caseII are shown in figure (14-A) at Ra= $7*10^{7}$. When the frequency is fr=2Hz, the time-average Nusselt numbers at vertical close to the horizontal at initial stage. Due to frequency increases to fr=4Hz, at vertical vibration, which the time-average Nusselt numbers begin to exceed that the horizontal vibration, as the frequency increases to fr=8Hz , the time-average Nusselt numbers returned to close to the horizontal vibrational motion. The variations of the time-averaged Nusselt numbers $\overline{Nu}$ at Ra= 7×10^{7} for descending frequencies case III are shown in figure (14-B). As the frequency decreased gradually and close to that of vertical vibration finally, must of the average Nusselt number at vertical vibration motion are smaller than that horizontal vibration, oppositely, the case II for ascending frequencies. Similarly at Ra= 4×10^{8} for case II for ascending frequencies(3,6and9)Hz, the comparison between the vertical and horizontal

vibrational motions are shown in figure(15-A). The variations of time-averaged Nusselt numbers $\overline{Nu}$ at vertical are larger than horizontal vibrational motion completely. For frequency (fr=3Hz) at initial stage, the average Nusselt number at vertical close to horizontal vibrational motion.

The variations of the average Nusselt numbers $\overline{Nu}$ with time τ at Ra= 4×10^8 for caseIII descending frequencies (9,6and3)Hz and comparison between the vertical and horizontal vibrational motions are shown in figure(15-B). This case completely opposite the case II and the average Nusselt numbers at vertical motion smaller than that horizontal motion. As a result, the interaction of both motions mentioned above leads the magnitude of time-average Nusselt number vary from small to large as the effect of vibrational frequency. From figures (14AandB), it is found that the mean value of the time-varying $\overline{Nu}$ is slightly increased by the vertical vibrational direction of the enclosure at caseII(ascending frequencies), as compared with that of the horizontal vibration of enclosure at Ra=7×10^7. At the case III(descending frequencies) the mean value of the time-varying $\overline{Nu}$ is slightly increased by the horizontal vibrational direction of the enclosure, as compared with that of vertical vibration at the same case and same Rayleigh number. At the same cases (ascending case II and descending case III), as Ra number increases to 4×10^8 shown in figures (15AandB), it is noted that the mean value of the time-varying $\overline{Nu}$ is much larger than that indicated at Ra=7×10^7 by the vertical vibrational direction of enclosure of caseII as compared with that of the horizontal vibrational direction. At the case III(descending frequencies) the mean value of the time-varying $\overline{Nu}$ is much larger increased by the horizontal vibrational direction of the enclosure, as compared with that of vertical vibration at the same case and same Rayleigh number. At Ra=7×10^7, under vibratory conditions the boundary layer was either completely laminar or underwent transient from laminar to turbulent flow at some fixed distance up the hot and cold wall. In contrast at Ra=4×10^8, the boundary layer under vibratory conditions indicated that a turbulent boundary layer existed over the entire surface of the plates in vicinity of frequencies (3and9) Hz. By increasing Rayleigh number from 7×10^7 to4×10^8, the boundary layer will be thicker. The thickness will be different from vibrational frequency to another.

CONCLUSIONS

In this study, the effects of vibration on natural convection in square enclosure in two directions horizontal and in vertical are investigated numerically. the variations of frequency(2,4and8) Hz at Ra= 7×10^7 and (3,6and9)Hz at Ra=4×10^8 are considered with different cases. CaseI (reaches to steady state and then begins the effect of vibration at each frequency), caseII and caseIII(begin the effect of vibration from the transient at ascending and descending frequencies respectively). The mean conclusions could be summarized as follows:

1. Results show that unsteady flow recirculation is formed and varied with time for the low-frequency situation. Then, the thermal field experiences a remarkable change as the vibration frequency elevated.
2. At case I , natural convection heat transfer of a square enclosure subjected to a vibration motion in vertical direction under certain combination of frequency is possibly larger than that of stationary state at both Ra= 7×10^7 and Ra=4×10^8.
3. At case I, natural convection heat transfer of square enclosure subjected to a vibration motion in horizontal direction under certain combination of frequency is possibly smaller than that of stationary state for both Ra= 7×10^7 and Ra=4×10^8.
4. At case II (ascending frequency), the time-average Nusselt numbers $\overline{Nu}$ subjected to a vibration motion in vertical are larger than the horizontal at both Ra= 7×10^7 and Ra=4×10^8.
5. 4. At case III (descending frequency), the time-average Nusselt numbers $\overline{Nu}$ subjected to a vibration motion in horizontal are larger than the vertical at both Ra= 7×10^7 and Ra=4×10^8.

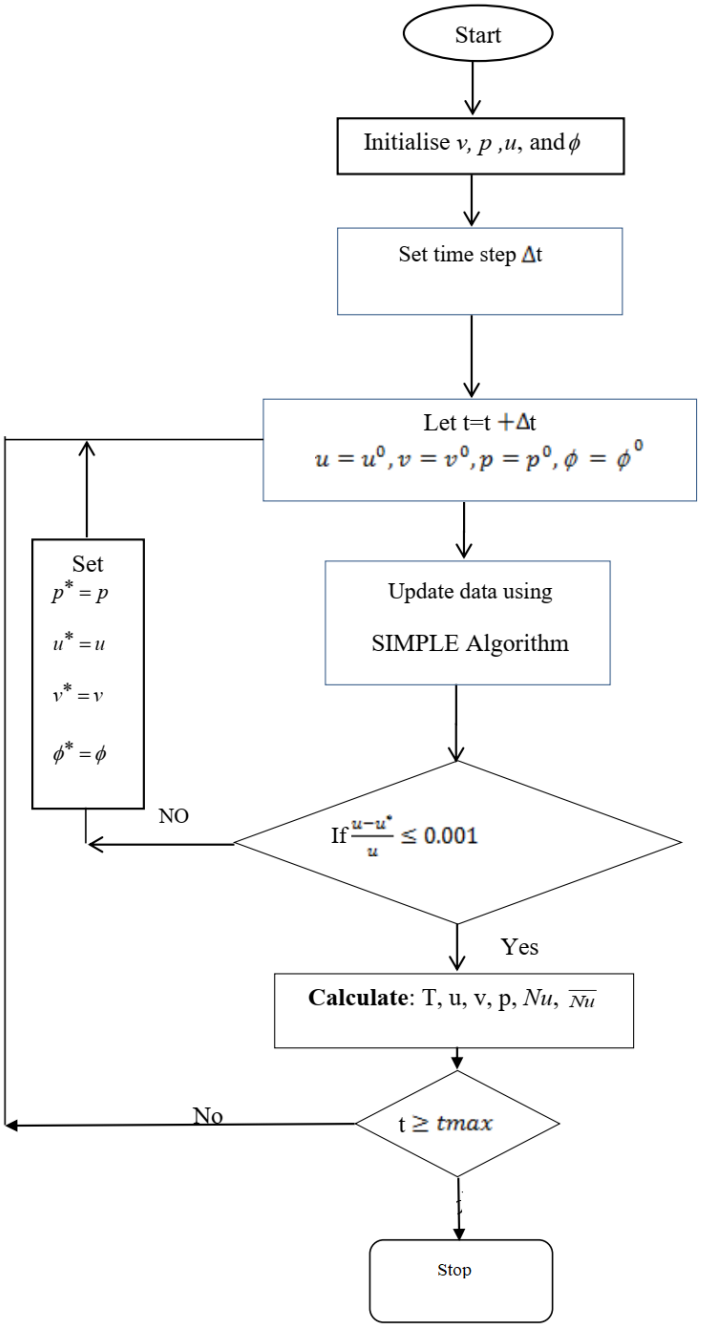

Fig. (2) . Flow chart for present work

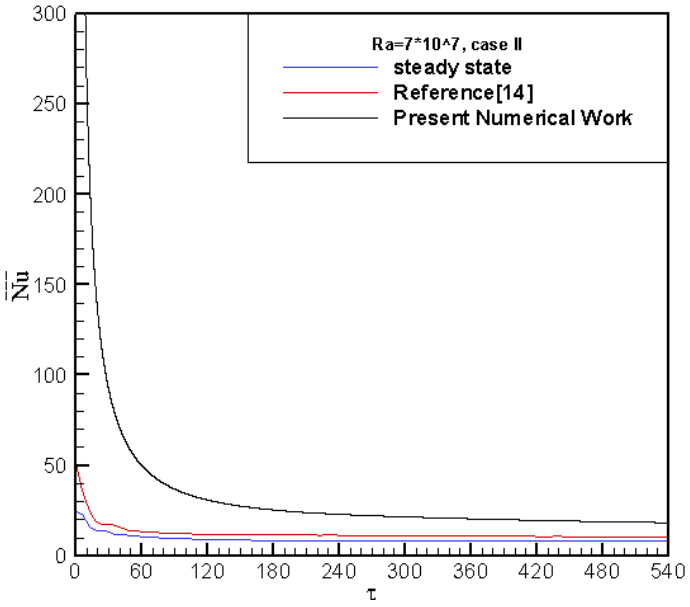

(a) aseII

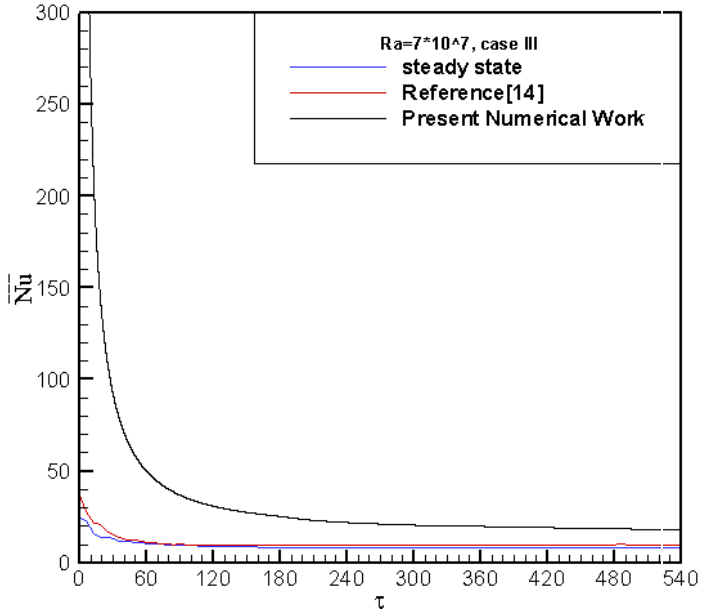

(b) caseIII at Ra7× 10^7,

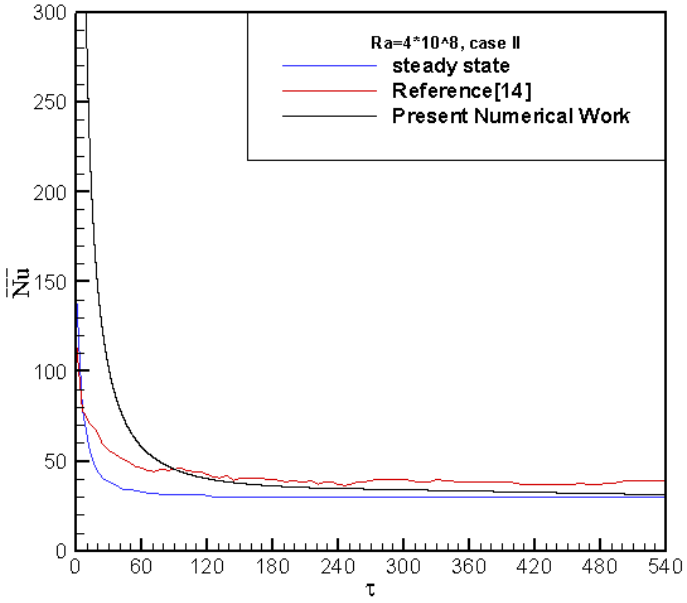

(c) caseII

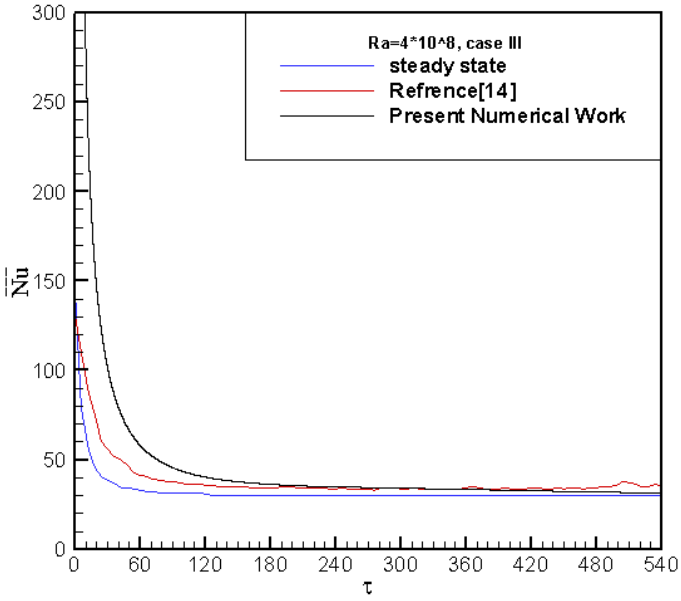

(d) caseIII Ra=4× 10^8

Fig. (3A). Comparison of the variation of the average Nusselt number for different time step

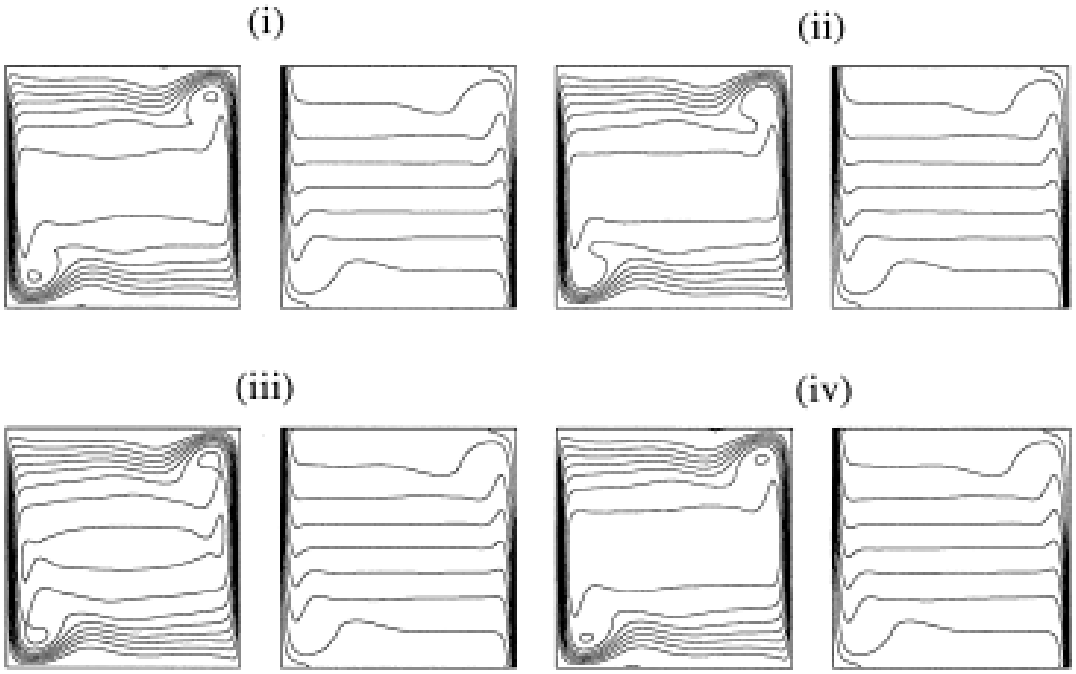

(B)

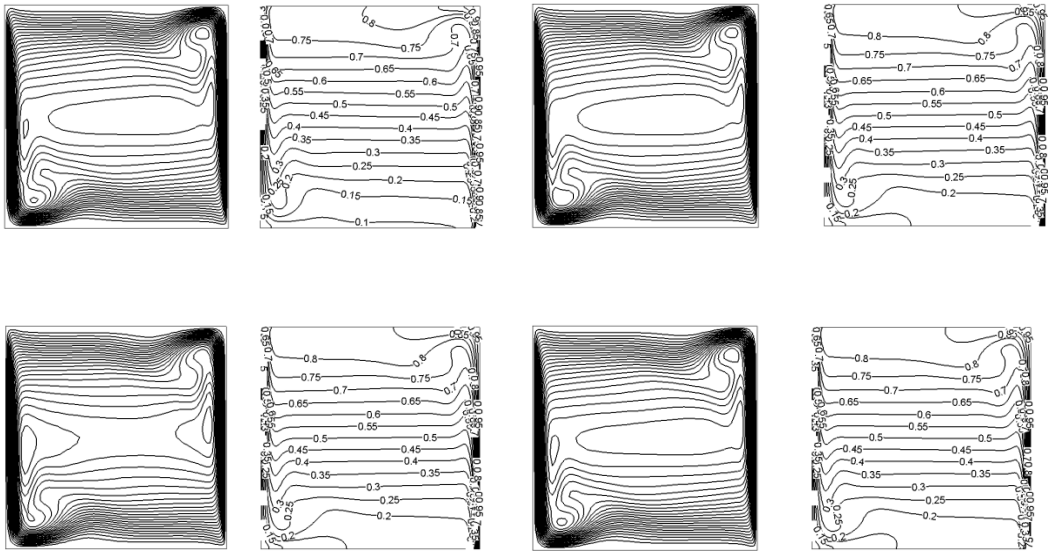

Fig. (4). Comparison of the Previous Work (Ki Hyun Kim ***et al***. ,2001) at (A) and Present Results at (B), at vertical vibrational direction flow pattern (in the left box) and temperature fields (in the right box) are shown in each pair of the boxes, Ra =10^7, ω=0.66. Time instants are(i) $\tau = 100$, (ii)$\tau = 200$,(iii)400and(iv) τ=600.

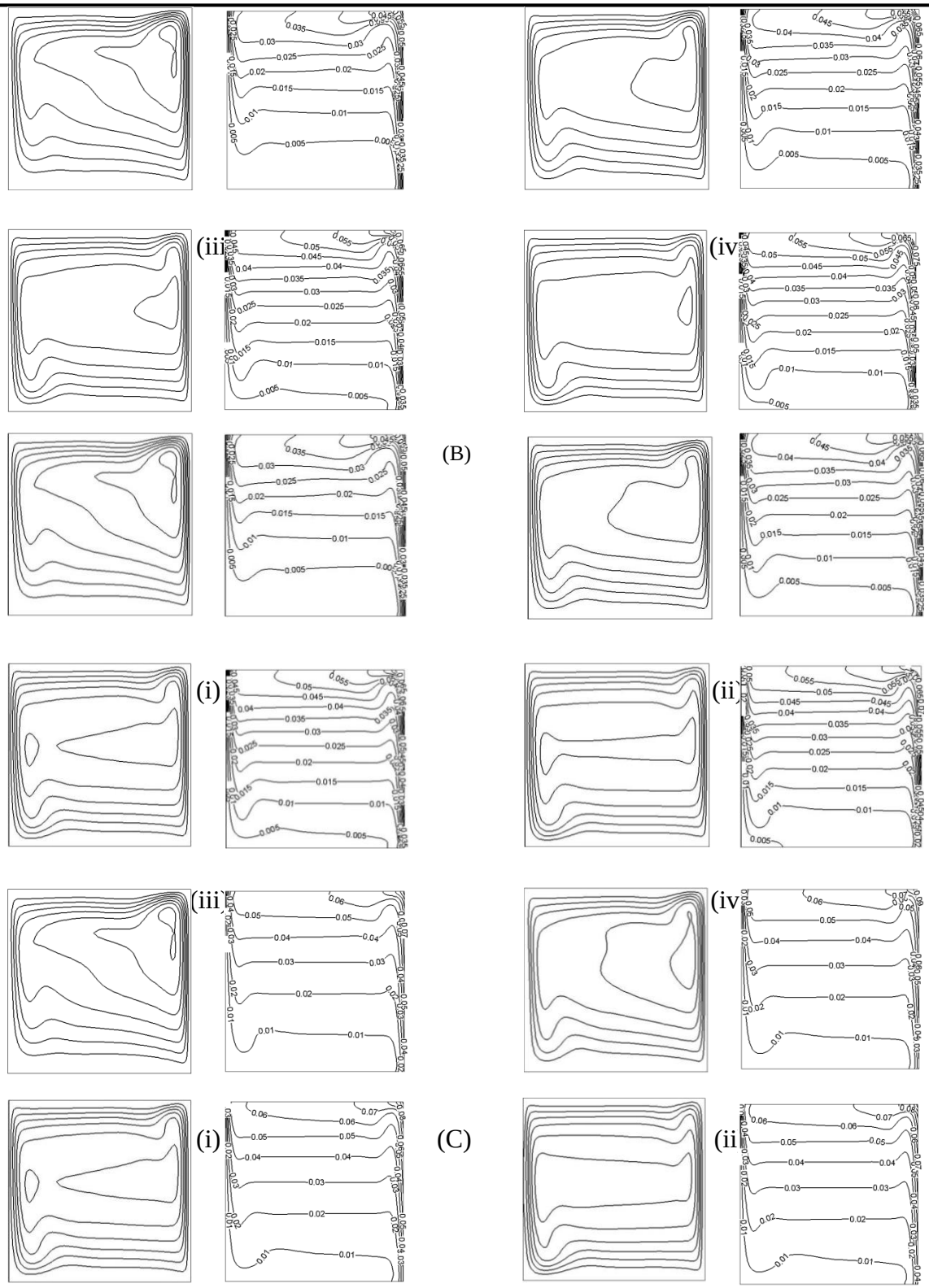

Fig. (5). Flow pattern (in the left box) and temperature fields (in the right box) in vertical directional vibration are shown in each pair of the boxes, case I, Ra =7×10^7. (A) $f_r = 2Hz$, (B) $f_r = 4Hz$, (C) $f_r = 8Hz$. Dimensionless time instants are (i) $\tau = 100$,, (ii) $\tau = 200$,, (iii) $\tau = 400$,and (iv) $\tau = 600$, after a steady state thermal the oscillation has been established.

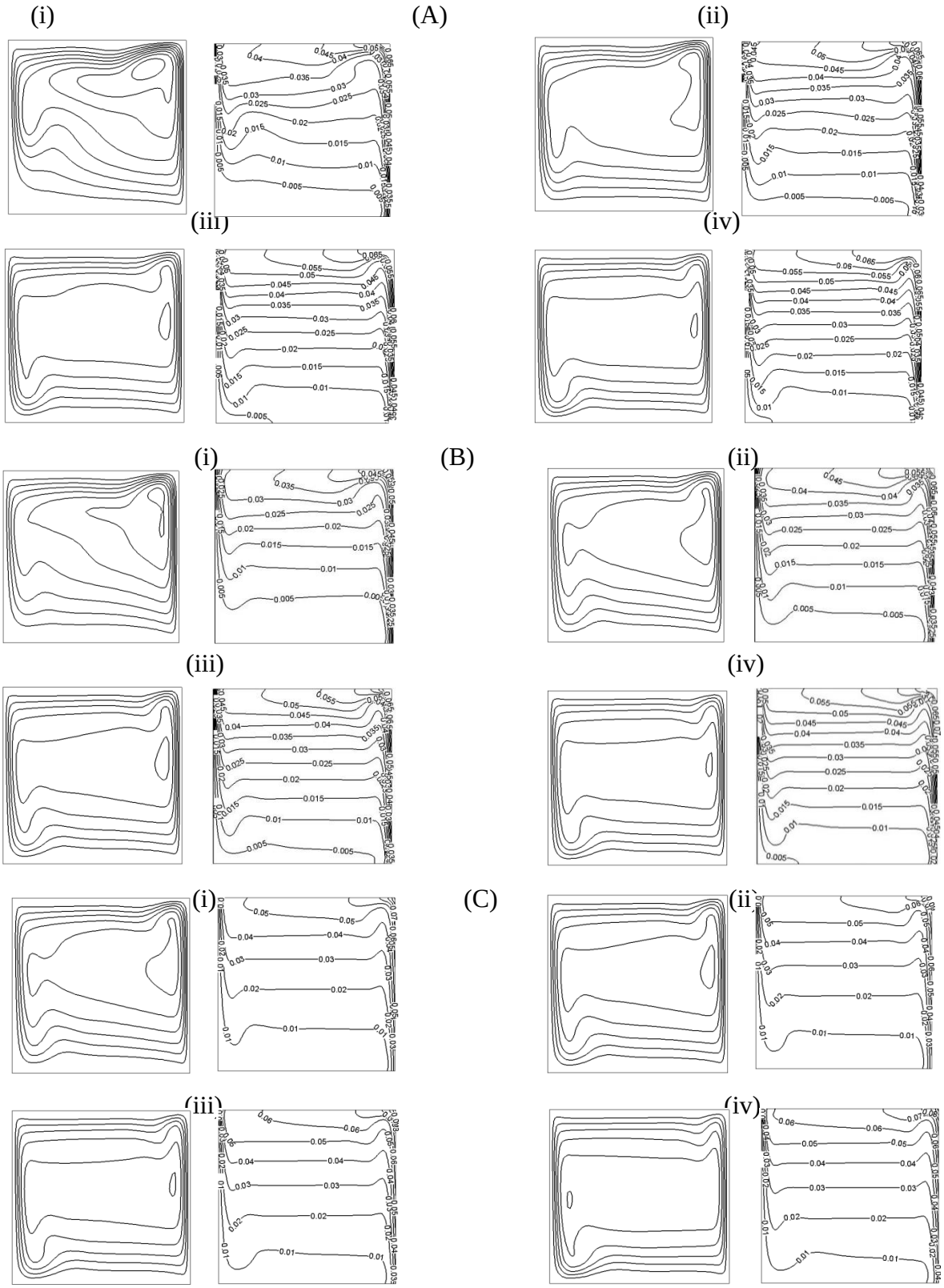

Fig.(6). Flow pattern (in the left box) and temperature fields (in the right box) in horizontal directional vibration are shown in each pair of the boxes, case I, Ra $=7 \times 10^7$. (A) $f_r = 2Hz$, (B) $f_r = 4Hz$, (C) $f_r = 8Hz$. Dimensionless time instants are (i) $\tau = 100$,, (ii) $\tau = 200$,, (iii) $\tau = 400$,and (iv) $\tau = 600$, after a steady state thermal the oscillation has been established.

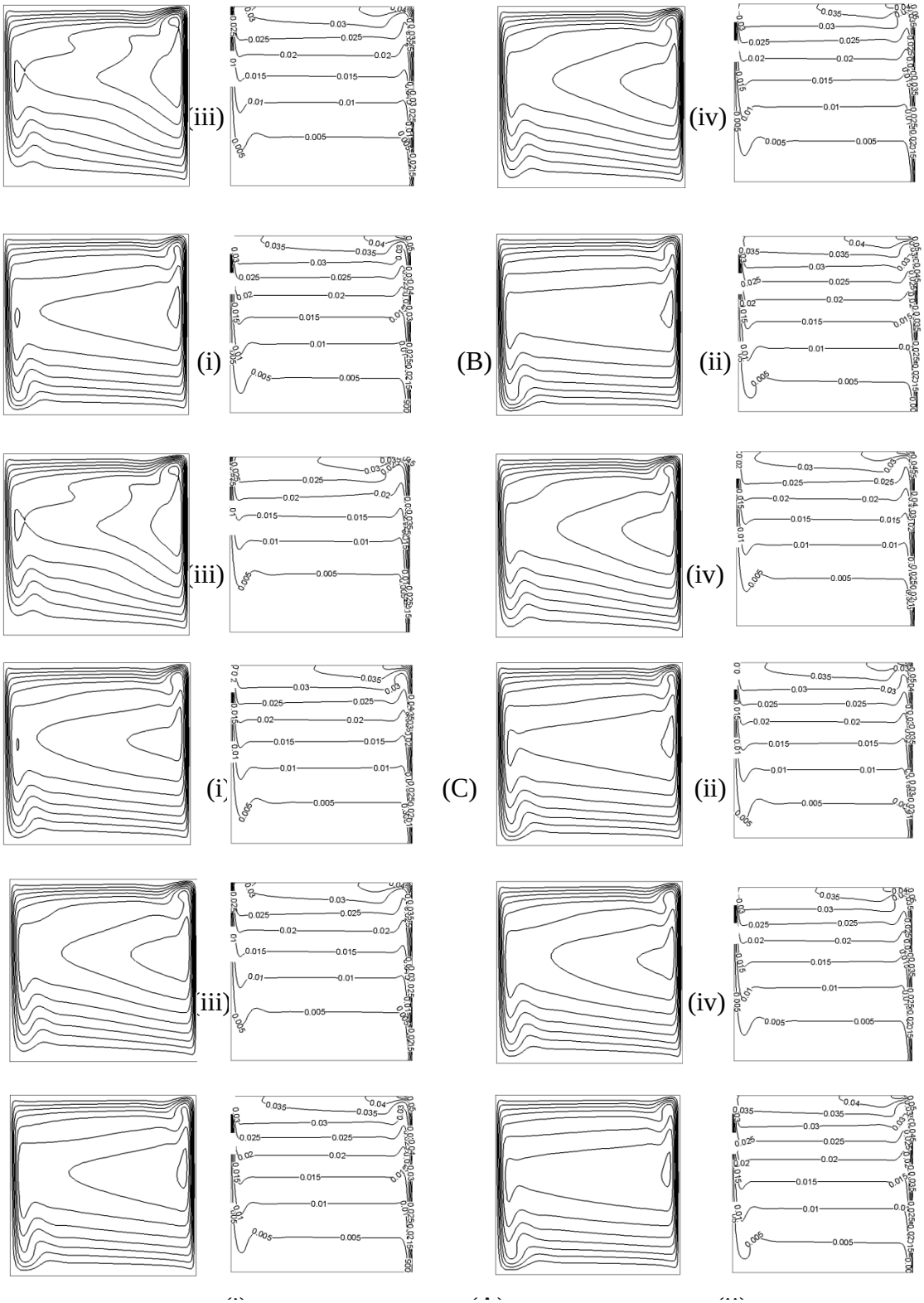

Fig. (7). Flow pattern (in the left box) and temperature fields (in the right box) in vertical directional vibration are shown in each pair of the boxes, case I, Ra =4×10^8. (A) $f_r = 3Hz$ (B) $f_r = 6Hz$ (C) $f_r = 9Hz$. Dimensionless time instants are (i) $\tau = 100$, (ii) $\tau = 200$ (iii) $\tau = 400$ and (iv) $\tau = 600$ after a steady state thermal the oscillation has been established.

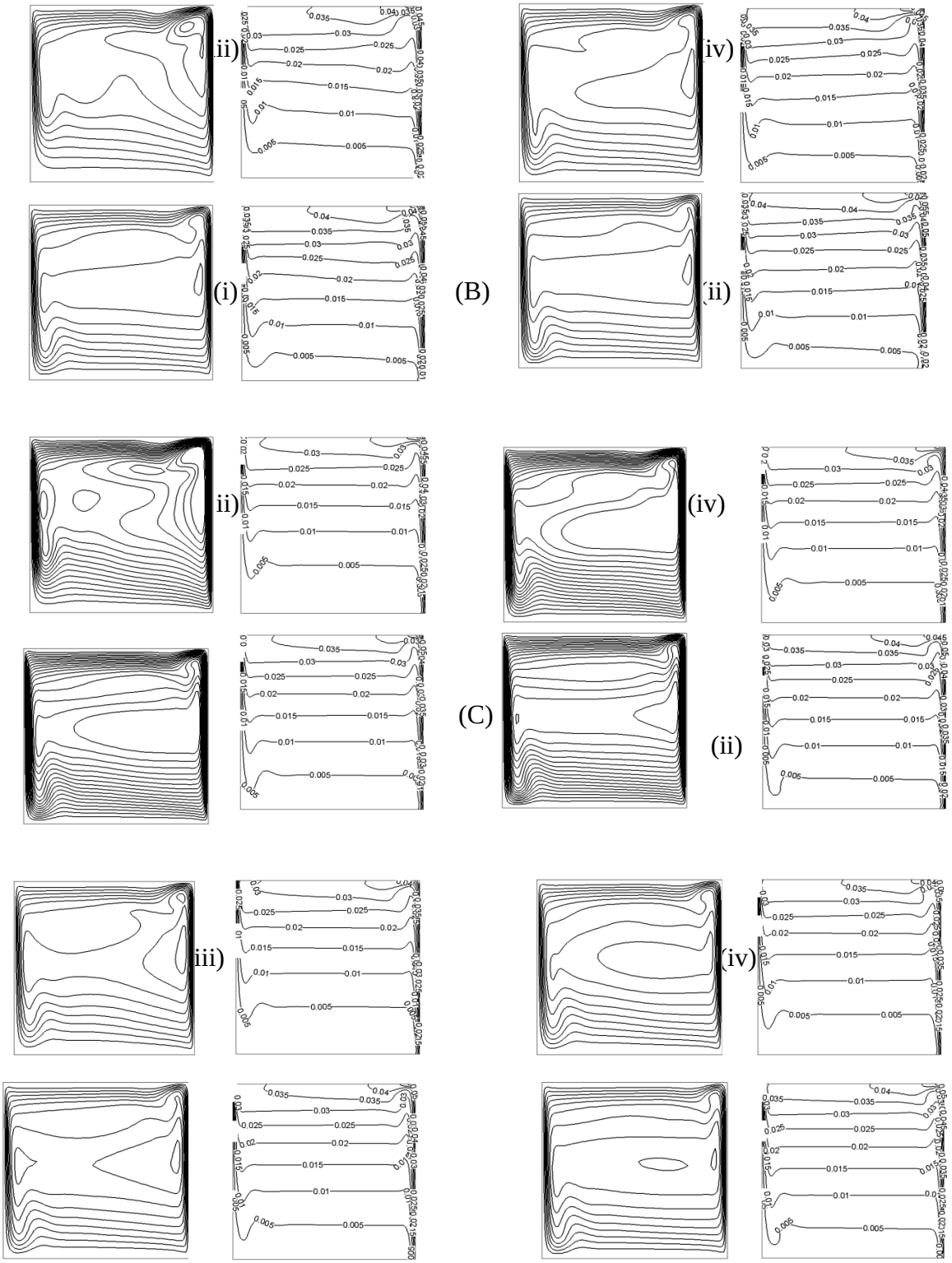

Fig. (8). Flow pattern (in the left box) and temperature fields (in the right box) in horizontal directional vibration are shown in each pair of the boxes, case I, Ra $=4 \times 10^8$. (A) $f_r = 3Hz$ (B) $f_r = 6Hz$ (C) $f_r = 9Hz$. Dimensionless time instants are (i) $\tau = 100$, (ii) $\tau = 200$ (iii) $\tau = 400$ and (iv) $\tau = 600$ after a steady state thermal the oscillation has been established.

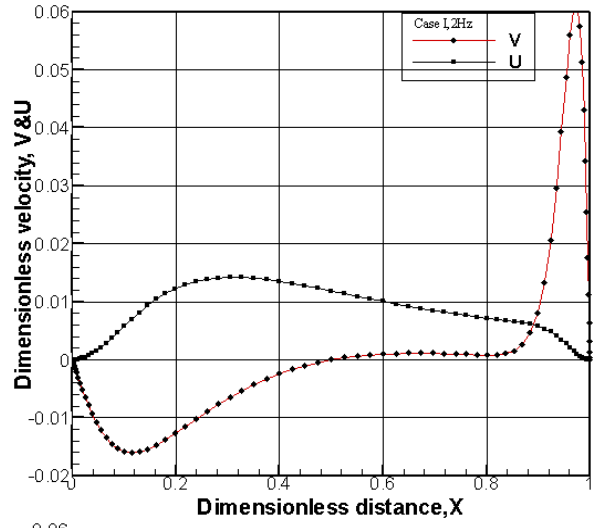

(A)

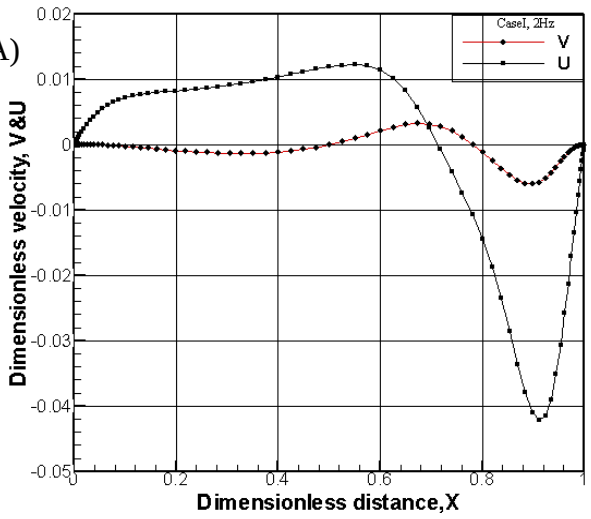

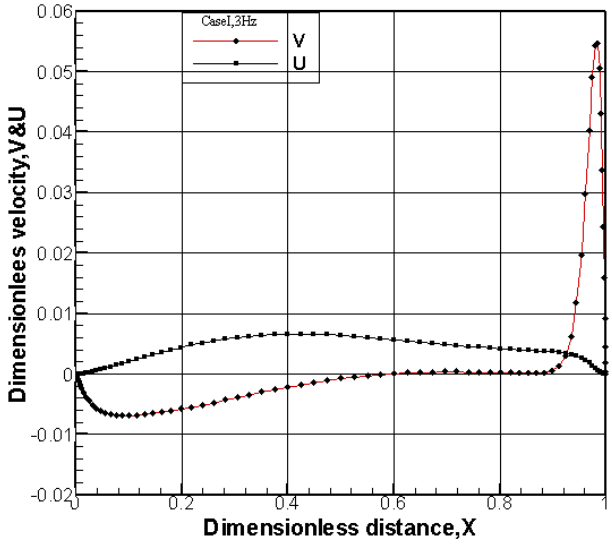

(B)
(b

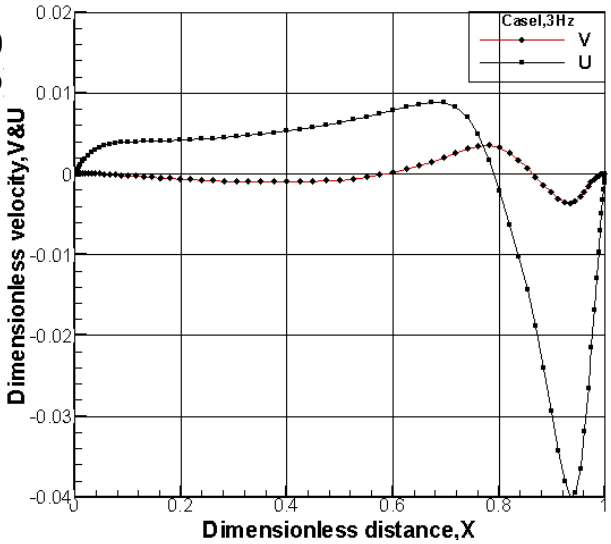

(c)

(d)

(c) at vertical directional vibration, (d) at horizontal directional vibration case I at Ra=4×10^{8}

Fig.(9) velocity distribution at mid plane

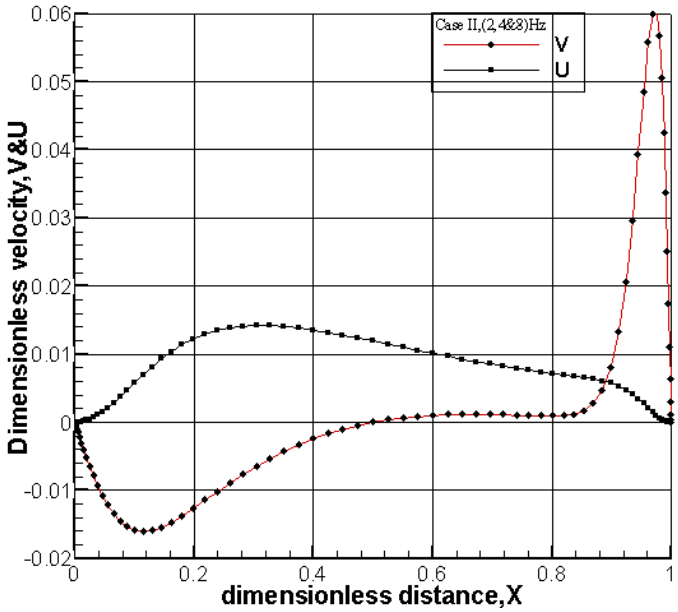

(A)

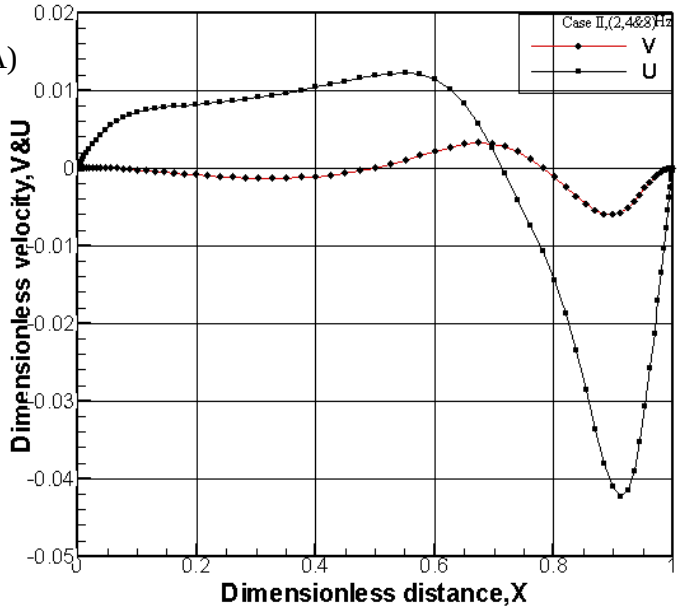

(a)Vertical vibration

(b) horizontal vibration vibration case II at Ra=4×10^{7}

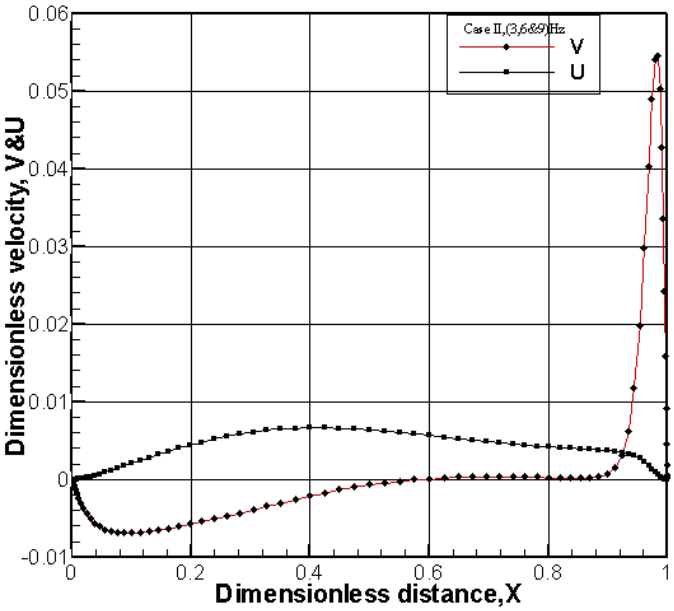

(B)

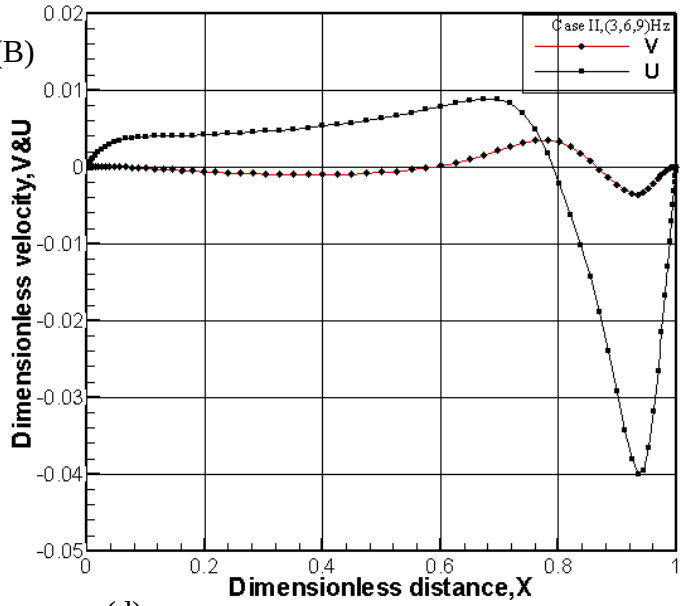

(d)

(c)at vertical direction vibration

(d) at horizontal directional vibration caseIIat Ra=4×10^{8}

Fig.(10) velocity distribution at mid plane

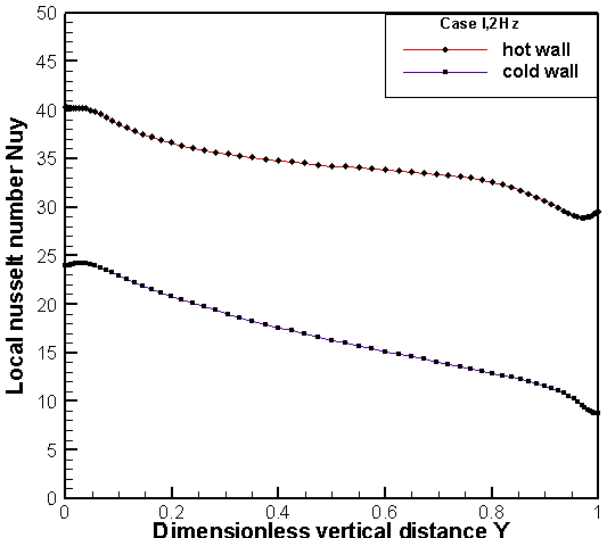

(a) at vertical directional vibration,

(A)

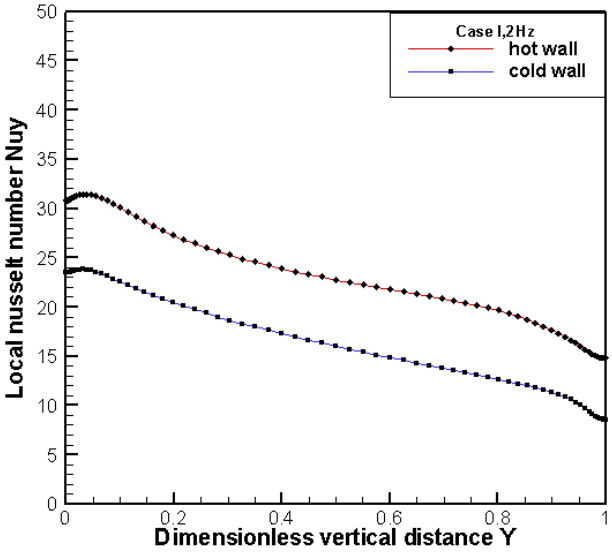

(b) at horizontal directional vibration case I at Ra=7×10^7

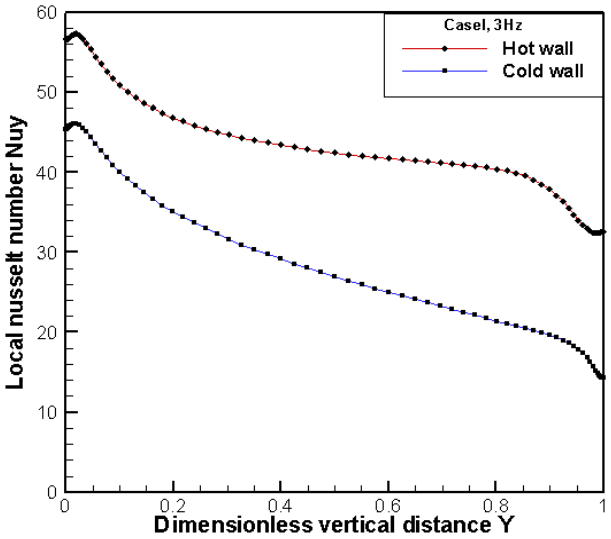

(B)

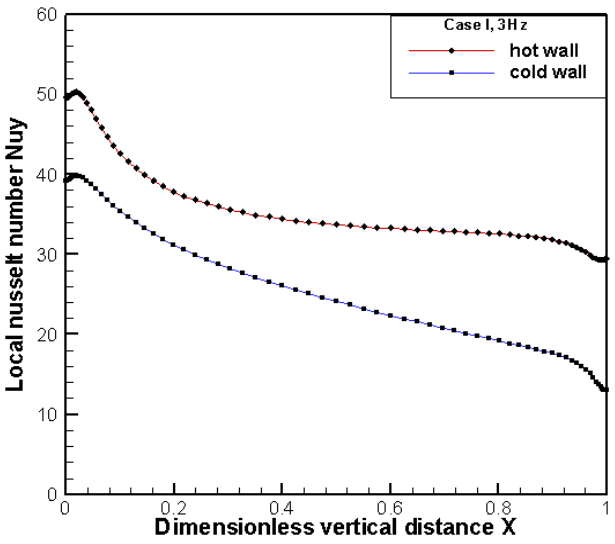

(c) at vertical directional vibration, (d) at horizontal directional vibration case I at Ra=4×10^8

Fig.(11) local Nusselt number distributions on the hot and cold walls

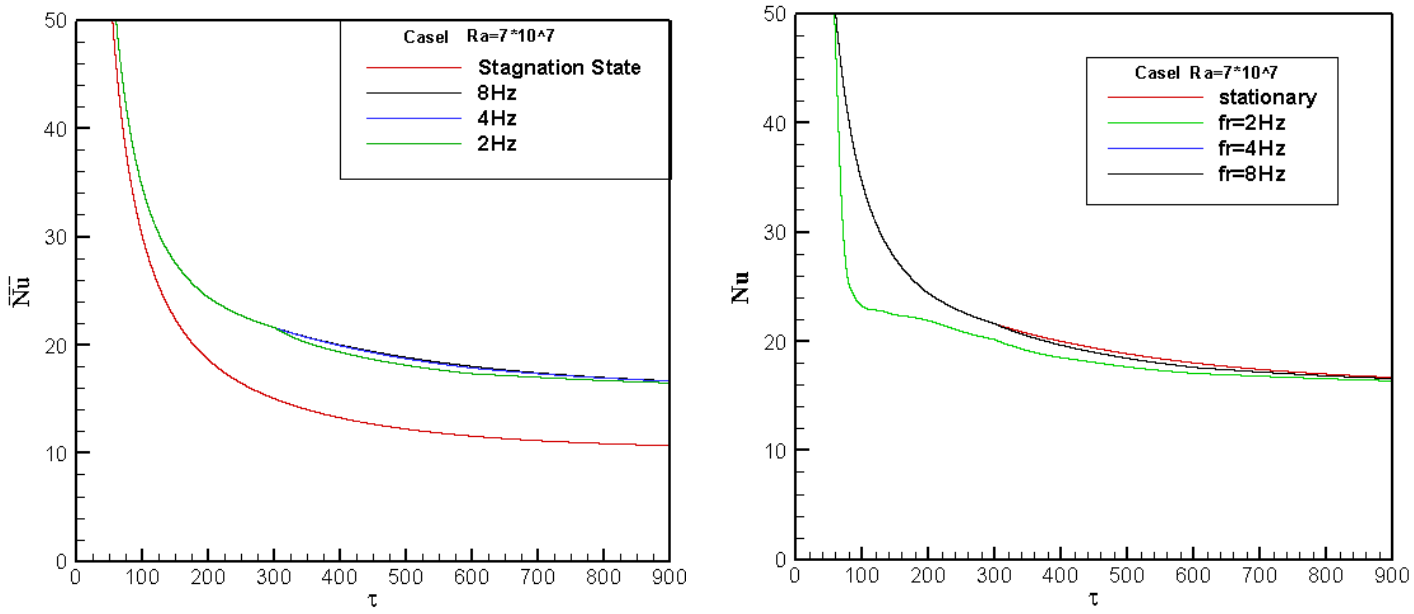

(a) vertical directional vibration (b) horizontal directional vibration caseI at Ra=7×10^{7}.

Fig.(12). Comparison of the variation of the average Nusselt number for different time step

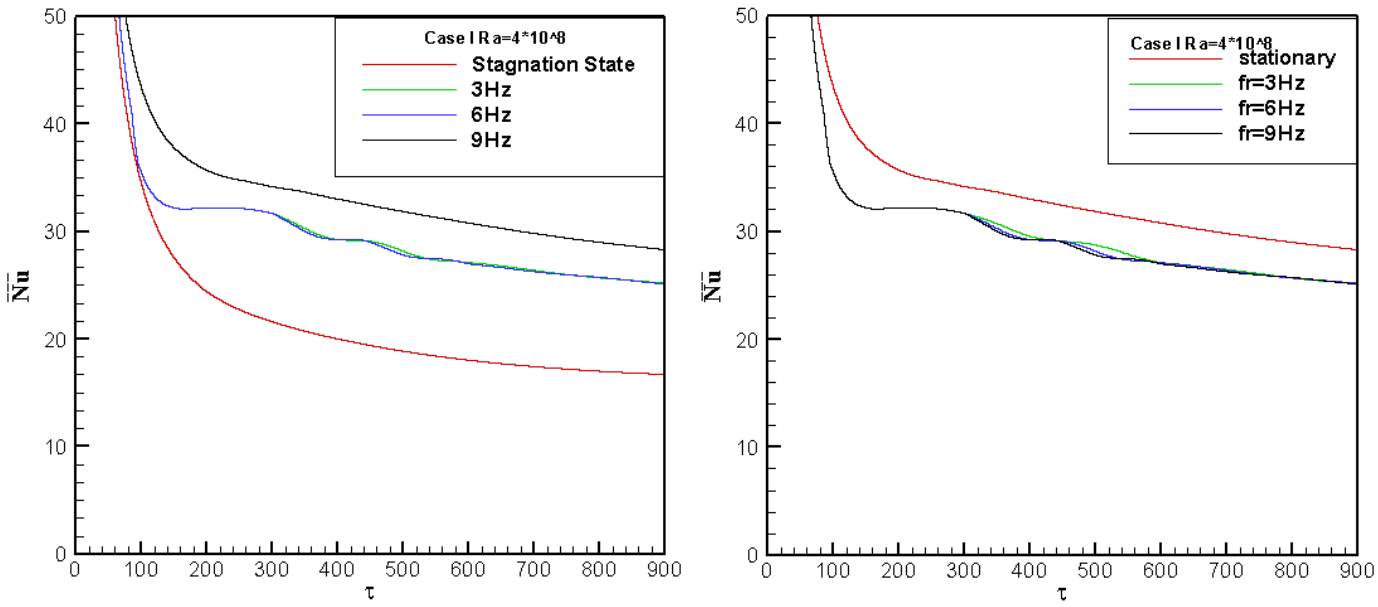

(a) at vertical directional vibration (b) at horizontal directional vibration caseI at Ra =4×10^{8}.

Fig.(13). Comparison of the variation of the average Nusselt number for different time step.

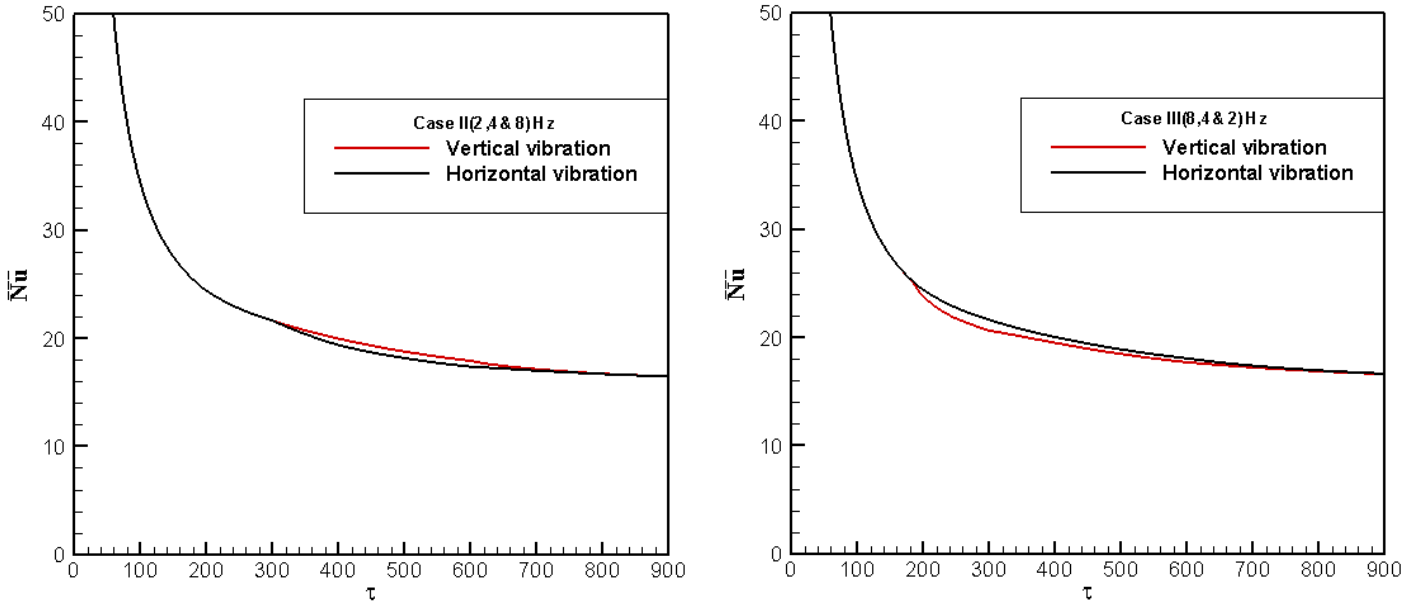

(a) -case II (b) case III at Ra =7×10^7.

Fig.(14). Comparison of the variation of the average Nusselt number between vertical and horizontal vibrational direction for different time step.

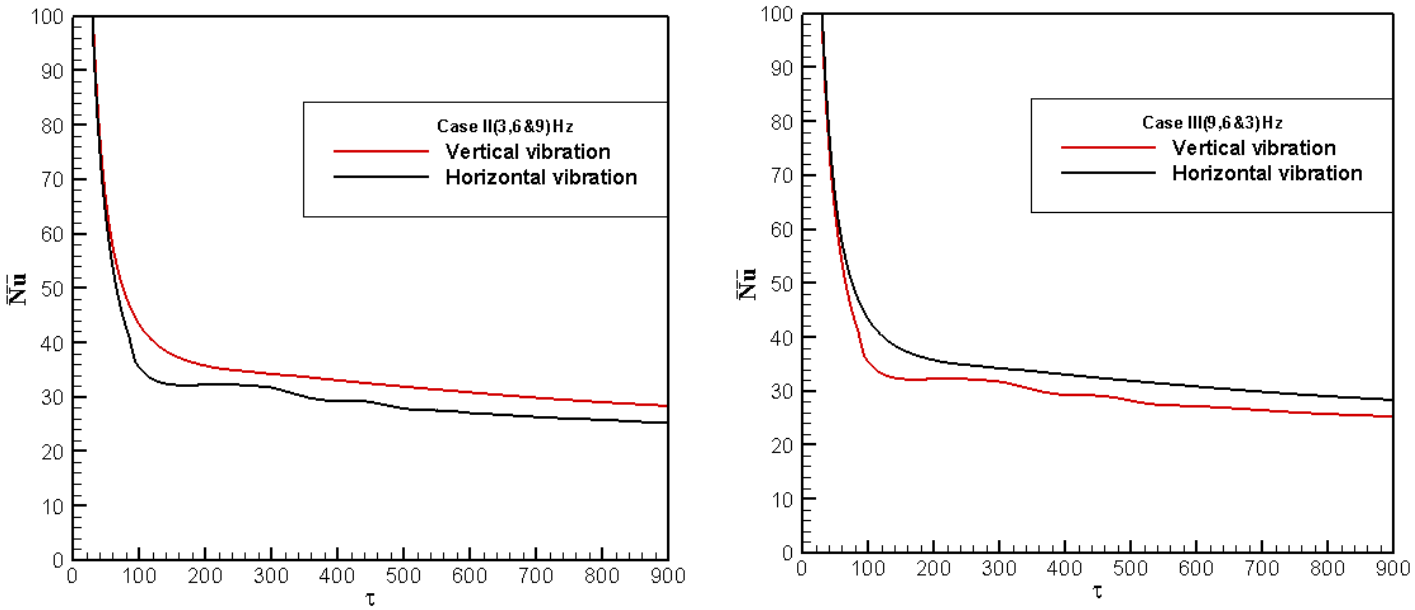

(a)caseII (b) caseIII at Ra=4×10^8

Fig.(15). Comparison of the variation of the average Nusselt number between vertical and horizontal vibrational direction for different time step.

REFERENCES

A. A. Ivanova, " Influence of vibrations of the unsteady state convective heat transfer in a cylindrical cavity", Heat Transfer-Sov. Res. 20, pp. 248-251, (1988).

Adel M. Salh, Kays A.Al-Taey, Baydaa Kh. Khudhair, "Experimental Study of Natural Convection Heat Transfer in an Enclosed Vibration Cavity", IISTE Journal of Energy Technologies and Policy, ISSN 2224-3232, Vol.4, No.10, 2014.

Amirhossein Ahadi, Armin Kianian andM. Ziad Saghir, "Heat and mass transport phenomena under the influence of vibration using a new aided image processing approach", International Journal of Thermal Sciences 75, (2014), pp. 233-248.

Baydaa Khalil Khudhair, "The Effect of Vibration on Natural Convection Heat Transfer in an Enclosed Cubic Cavity", MSc Thesis, Depatment of Mechanical Engineering, University of Technology,(2014).

E. Papanicolaou and V. Belessiotis, **"**Double-diffusive natural convection in an asymmetric trapezoidal enclosure: unsteady behavior in the laminar and the turbulent-flow regime", International Journal of Heat and Mass Transfer 48, (2005), pp.191–209.

Frank T. Ferguson and Lembit U. Lilleleht, "Thermovibrational convection in a verticalcylinder", Int. J. Heat Mass Transfer. Vol. 39, No. 14, pp. 2895-2906, 1996.

G. Barakos, E. Mitsoulis and D. Assimacopoulos, "Natural Convection Flow in a Square Cavity Revisted: Laminar and Turbulent Models with Wall Functions", International Journal for Numerical Methods in Fluids, Vol. 18, pp. 695-719, (1994).

Hideshi Ishida, Kohei Yamamoto, Satoshi Nishihara, Toshinori Oki and Genta Kawahara, "Forced oscillations, optimal forcing and resonance of thermal convection under small, time-varying forcing", International Journal of Heat and Mass Transfer 55, (2012), pp. 6618–6631.

Ki Hyun Kim, Jae Min Hyun and Ho Sang Kwak, "Buoyant convection in a side-heated cavity under gravity and oscillations", International Journal of Heat and Mass Transfer 44 (2001) 857-86.

M. Wadih and B. Roux, Natural convection in a long vertical cylinder under gravity modulation, J. Fluid Mech. 193, 391415 (1988).

P. D. Richardson, Effects of sound and vibrations on heat transfer, AMR 20, 201-217 (1967).
R. E. Forbes, C. T. Carley and C. J. Bell, **"Vibration effects on convective heat transfer in enclosures"** J. Heat Transfer 92 (1970), pp 429-438.

Sohail Anwar, "Natural Convection Flow in Parallel-Plate Vertical Channels", MSc Thesis, Department of Mechanical Engineering, KING FAHD UNIVERSITY of PETROLEUM and MINERALS, (2003).

S.V.Patankar,Numerical Heat Transfer and Fluid Flow,Hemisphere/McGraw-Hill, New

York, 1980.
Wu-Shung Fu and Chien-Ping Huang, "Effects of a vibrational heat surface on natural convection in a vertical channel flow", International Journal of Heat and Mass Transfer 49, (2006), pp. 1340–1349.

Wu Shung Fu and Wen Jiann Shieh, "A study of thermal convection in an enclosure induced simultaneously by gravity and vibration", Int. J. Heat Mass Transfer., Vol. 35, No. 7, pp. 1695-1710, (1992).
Wu Shung Fu and Wen Jiann Shieh, "Transient thermal convection in an enclosure induced simultaneously by gravity and vibration", Int. J. Heat Mass Transfer. Vol. 36, No. 2, pp. 437-452, (1993).

Y. Kamotani, A. Prasad and S. Ostrach. Thermal convection in an enclosure due to vibrations aboard spacecraft, AIAA J. 19,5l l-516 (1981).

Yuan Zhao , "Numerical Analysis of Thermal and Thermosolutal Vibrational Convection and its Effects on Heat and Mass Transport", Ph.D. Thesis, Department of Mechanical and Aerospace Engineering University of Case WESTERN Reserve